MAGIC Upper Limits for two Milagro-detected, Bright Fermi Sources in the Region of SNR G65.1+0.6

J. Aleksić[a], L. A. Antonelli[b], P. Antoranz[c], M. Backes[d], J. A. Barrio[e], D. Bastieri[f],
J. Becerra González[g,h], W. Bednarek[i], A. Berdyugin[j], K. Berger[g], E. Bernardini[k],
A. Biland[l], O. Blanch[a], R. K. Bock[m], A. Boller[l], G. Bonnoli[b], P. Bordas[n], D. Borla
Tridon[m], V. Bosch-Ramon[n], D. Bose[e], I. Braun[l], T. Bretz[o], M. Camara[e], E. Carmona[m],
A. Carosi[b], P. Colin[m], J. L. Contreras[e], J. Cortina[a], S. Covino[b], F. Dazzi[p,*], A. De Angelis[p],
E. De Cea del Pozo[q], B. De Lotto[p], M. De Maria[p], F. De Sabata[p], C. Delgado Mendez[g,**],
A. Diago Ortega[g,h], M. Doert[d], A. Domínguez[r], D. Dominis Prester[s], D. Dorner[l],
M. Doro[f], D. Elsaesser[o], M. Errando[a], D. Ferenc[s], M. V. Fonseca[e], L. Font[t], R. J. García
López[g,h], M. Garczarczyk[g], M. Gaug[g], G. Giavitto[a], N. Godinović[s], D. Hadasch[q],
A. Herrero[g,h], D. Hildebrand[l], D. Höhne-Mönch[o], J. Hose[m], D. Hrupec[s], T. Jogler[m],
S. Klepser[a], T. Krähenbühl[l], D. Kranich[l], J. Krause[m], A. La Barbera[b], E. Leonardo[c],
E. Lindfors[j], S. Lombardi[f], F. Longo[p], M. López[f], E. Lorenz[l,m], P. Majumdar[k],
G. Maneva[u], N. Mankuzhiyil[p], K. Mannheim[o], L. Maraschi[b], M. Mariotti[f], M. Martínez[a],
D. Mazin[a], M. Meucci[c], J. M. Miranda[c], R. Mirzoyan[m], H. Miyamoto[m], J. Moldón[n],
A. Moralejo[a], D. Nieto[e], K. Nilsson[j], R. Orito[m], I. Oya[e], R. Paoletti[c], J. M. Paredes[n],
S. Partini[c], M. Pasanen[j], F. Pauss[l], R. G. Pegna[c], M. A. Perez-Torres[r], M. Persic[p,v],
L. Peruzzo[f], J. Pochon[g], F. Prada[r], P. G. Prada Moroni[c], E. Prandini[f], N. Puchades[a],
I. Puljak[s], I. Reichardt[a], R. Reinthal[j], W. Rhode[d], M. Ribó[n], J. Rico[w,a], M. Rissi[l],
S. Rügamer[o], A. Saggion[f], K. Saito[m], T. Y. Saito[m], M. Salvati[b], M. Sánchez-Conde[g,h],
K. Satalecka[k], V. Scalzotto[f], V. Scapin[p], C. Schultz[f], T. Schweizer[m], M. Shayduk[m],
A. Sierpowska-Bartosik[i], A. Sillanpää[j], J. Sitarek[m,i], D. Sobczynska[i], F. Spanier[o], S. Spiro[b],
A. Stamerra[c], B. Steinke[m], J. Storz[o], N. Strah[d], J. C. Struebig[o], T. Suric[s], L. Takalo[j],
F. Tavecchio[b], P. Temnikov[u], T. Terzić[s], D. Tescaro[a], M. Teshima[m], D. F. Torres[w,q],
H. Vankov[u], R. M. Wagner[m], Q. Weitzel[l], V. Zabalza[n], F. Zandanel[r], R. Zanin[a],

klepser@ifae.es, decea@ieec.uab.es

ABSTRACT

We report on the observation of the region around supernova remnant G65.1+0.6 with the stand-alone MAGIC-I telescope. This region hosts the two bright GeV gamma-ray sources 1FGL J1954.3+2836 and 1FGL J1958.6+2845. They are identified as GeV pulsars and both have a possible counterpart detected at about 35 TeV by the Milagro observatory. MAGIC collected 25.5 hours of good quality data, and found no significant emission in the range around 1 TeV. We therefore report differential flux upper limits, assuming the emission to be point-like ($\leq 0.1°$) or within a radius of $0.3°$. In the point-like scenario, the flux limits around 1 TeV are at the level of 3% and 2% of the Crab Nebula flux, for the two sources respectively. This implies that the Milagro emission is either extended over a much larger area than our point spread function, or it must be peaked at energies beyond 1 TeV, resulting in a photon index harder than 2.2 in the TeV band.

Subject headings: pulsars: individual(PSR J1957+2831, LAT PSR J1954+2836, LAT PSR J1958+2846) — ISM: supernova remnants

1

1. Introduction

In February 2009, the Fermi collaboration published a list of the most significant gamma-ray sources above 100 MeV, detected by the large area telescope (LAT) within 3 months of observation (Abdo et al. 2009b). The energy spectra of these sources often extend to several GeV, where at some point the steeply falling flux levels are too low to be detected by the limited detection area of a satellite instrument. Many of the LAT sources are hosted by our galaxy, and 34 of those are within the field of view of the Milagro gamma-ray observatory, which was located near Los Alamos, New Mexico (Abdo et al. (2009a) and references within). The Milagro collaboration, therefore, reinvestigated their previously gained skymap to look for counterparts to these GeV sources (Abdo et al. 2009a). The sensitivity of the instrument peaks in the energy range $10 - 50$ TeV, although it ultimately depends on the energy spectrum and the declination of the source. Due to the reduced trial factor, 14 new Milagro sources could be claimed with confidence levels above $3\,\sigma$.

Two of these Milagro-detected Fermi bright sources are in the vicinity of G65.1+0.6, a faint supernova remnant (SNR) first reported by Landecker et al. (1990). Tian & Leahy (2006) suggested its distance to be 9.2 kpc and a Sedov age of $40 - 140$ kyr. An association to the radio pulsar PSR J1957+2831 was suggested by Lorimer et al. (1998).

The gamma-ray emission in the region of G65.1+0.6 was first detected by the COS-B satellite (Swanenburg et al. 1981) as 2CG065+00, and later confirmed by the EGRET satellite (3EG J1958+2909) in Hartman et al. (1999), where a possible extension or multiple sources were denoted. As of now, the two sources could be detected as two individual sources by the LAT as 1FGL J1954.3+2836 and 1FGL J1958.6+2845, as reported in the first year catalog of Fermi sources (Abdo et al. 2010b). They were analysed and reported as gamma-ray pulsars found through blind search in Saz Parkinson et al. (2010), Abdo et al. (2009c) and Abdo et al. (2010a). Their periods (290 ms, 92.7 ms), spin-down luminosities (104.8×10^{34} ergs s^{-1}, 33.9×10^{34} ergs s^{-1}) and energy cutoffs (2.9 GeV, 1.2 GeV), but also the characteristic magnetic fields and ages (69.5 kyrs, 21 kyrs) lie in the average range of all Fermi pulsars. In the following, we will use the names J1954 and J1958 for these 1-year catalog sources, and J1954$_0$/J1958$_0$ to specifically refer to the 3-month bright source list positions.

The detections by Milagro revealed significances of $4.3\,\sigma$ for J1954$_0$ and $4.0\,\sigma$ for J1958$_0$ (Abdo et al. 2009a). Flux values are stated for a characteristic median energy of 35 TeV. The angular resolution of Milagro is about $0.4 - 1.0°$, so

[a]IFAE, Edifici Cn., Campus UAB, E-08193 Bellaterra, Spain

[b]INAF National Institute for Astrophysics, I-00136 Rome, Italy

[c]Università di Siena, and INFN Pisa, I-53100 Siena, Italy

[d]Technische Universität Dortmund, D-44221 Dortmund, Germany

[e]Universidad Complutense, E-28040 Madrid, Spain

[f]Università di Padova and INFN, I-35131 Padova, Italy

[g]Inst. de Astrofísica de Canarias, E-38200 La Laguna, Tenerife, Spain

[h]Depto. de Astrofisica, Universidad, E-38206 La Laguna, Tenerife, Spain

[i]University of Łódź, PL-90236 Lodz, Poland

[j]Tuorla Observatory, University of Turku, FI-21500 Piikkiö, Finland

[k]Deutsches Elektronen-Synchrotron (DESY), D-15738 Zeuthen, Germany

[l]ETH Zurich, CH-8093 Switzerland

[m]Max-Planck-Institut für Physik, D-80805 München, Germany

[n]Universitat de Barcelona (ICC/IEEC), E-08028 Barcelona, Spain

[o]Universität Würzburg, D-97074 Würzburg, Germany

[p]Università di Udine, and INFN Trieste, I-33100 Udine, Italy

[q]Institut de Ciències de l'Espai (IEEC-CSIC), E-08193 Bellaterra, Spain

[r]Inst. de Astrofísica de Andalucía (CSIC), E-18080 Granada, Spain

[s]Croatian MAGIC Consortium, Institute R. Boskovic, University of Rijeka and University of Split, HR-10000 Zagreb, Croatia

[t]Universitat Autònoma de Barcelona, E-08193 Bellaterra, Spain

[u]Inst. for Nucl. Research and Nucl. Energy, BG-1784 Sofia, Bulgaria

[v]INAF/Osservatorio Astronomico and INFN, I-34143 Trieste, Italy

[w]ICREA, E-08010 Barcelona, Spain

[*]supported by INFN Padova

[**]now at: Centro de Investigaciones Energéticas, Medioambientales y Tecnológicas

these values can be expected to hold also for the 1-year catalog positions of the sources, which are offset by $\leq 0.1°$. Since gamma-ray pulsars typically have energy cutoffs as low as several GeV, the Milagro signals, if real, can be expected not to be caused directly by the pulsars, but possibly by associated objects, such as a pulsar wind nebula (PWN) or, in the case of J1954, the shell of the SNR, which surrounds the pulsar. Gamma rays at TeV energies may also be produced in an interaction of the shell with a possibly coincident molecular cloud. This cloud may be located at the position of the infra-red source IRAS 19520+2759, which has associated CO line, H_2O and OH maser emission at a similar distance as the SNR (Arquilla & Kwok 1987).

The MAGIC telescopes use the Cherenkov imaging technique and are located on the Canary Island of La Palma (28.8°N, 17.8°W, 2220 m a.s.l.). It is the instrument with the lowest energy threshold among all Cherenkov telescopes. In single-telescope observations, as presented here, the nominal threshold in low zenith angle observations is 60 GeV (Albert et al. 2008a). It is therefore the instrument of choice to connect the upper ends of the Fermi spectra, which typically end at some tens of GeV, with the detections provided by Milagro at some tens of TeV. To bridge these spectra in the TeV range, and identify possible object associations for the Milagro signals were the main motivations for our investigation.

2. Observations

Motivated by the fact that $J1954_0$ was *not* marked as a pulsar in the initial Fermi Bright Source List, we observed $J1954_0$ as a main target in July and August 2009. The observations were carried out in false source tracking (wobble) mode (Fomin et al. 1994), which yielded two datasets with offsets of $\pm 0.4°$ in RA from this source, see Figure 1. The wobble position was altered every 20 min, and the data were taken at zenith angles between 0 and 43 degrees. At the time, the second MAGIC telescope was still under comissioning, so the analysis presented here used only the data from the stand-alone MAGIC-I telescope.

Quality selection cuts were applied to the event rate, the spread of hardware-sensitive shower image parameters, and few parameters that characterize the transparency of the atmosphere, such as the sky temperature and humidity. After all data selection cuts, 25.5 hours of high quality data were left for the analysis of J1954.

Besides this, we took advantage of the fact that J1958 is in the field of view of one of the two wobble positions. It could be analysed in a specific way described in the next section, yielding 13.8 hours of effective observation time.

3. Analysis and Results

The data were analysed in the MARS analysis framework (Moralejo et al. 2009), which is the standard software used in the analysis of MAGIC data. After the air shower images of the photomultiplier tube camera are calibrated, and times and charges of each pixel are extracted, a three-stage image cleaning is applied to filter out uncorrelated noise from the data acquisition electronics and the night sky background (Aliu et al. 2009). Shower image parameters are calculated, and the Random Forest method (Albert et al. 2008b) is used to derive estimators for the shower direction, its energy, and its likeliness to be of hadronic origin.

The observational setup described in the previous section requires a different analysis treatment of both sources. The main target of the observation, J1954, can be analysed using standard wobble analysis procedures. This means that the photon flux from the source is compared to the one on the opposite side of the camera (*anti*-source, solid squares in Figure 1). In this way, exposure inhomogeneities that can arise from imperfections in the photo multiplier tubes, trigger electronics or the signal transmission, cancel out, because both wobble positions were equally populated.

In the case of J1958, a wobble analysis, using only one of the two wobble positions, is not guaranteed to cancel out these inhomogeneities. Therefore, the analysis was done in ON/OFF manner, using the near wobble sample as ON-source data and the far wobble sample as OFF-source data (hollow squares in Figure 1). Having the OFF-source at the same position in relative camera coordinates as the source in the ON sample, the exposure inhomogeneities cancel out.

To test the presence of a gamma-ray signal, the distributions of squared angular distances (θ^2) between photon directions and the source positions

were used. In these θ^2-plots, a signal is expected to produce an excess where θ^2 approaches zero. However, the integrals over the expected signal regions of the θ^2 distributions agree, for both sources, well with the corresponding integrals done with respect to the OFF regions. Furthermore, the shapes of the ON and OFF distributions agree well with each other, and are sufficiently flat to exclude the unlikely case of an emission occuring by chance at both ON and OFF locations at a similar flux level, supressing the significance of the θ^2 comparison. Such a coincidence was also excluded by cross-checking the analysis using several OFF regions, and by thoroughly investigating the skymaps with different background estimation algorithms. Consequently, we report the absence of a significant signal for both sources.

Besides this analysis, which takes advantage of a-priori defined source locations, also a $2.8° \times 2.0°$ skymap of the area was investigated at different energy ranges. The trial factors implied by these searches were typically between 120 and 260, depending on the PSF, which is smaller for high energies. Taking into account these trials, no significant signal was found at any energy.

We convert our data into three differential flux upper limits for each source. To do so, the data was divided into three bins of estimated energy, delimited by 120 GeV, 375 GeV, 2.8 TeV and 12 TeV. For each bin, an *event number* upper limit is calculated from the above-mentioned θ^2-plots, at 95% confidence level (c.l.) after Rolke et al. (2005), and assuming an efficiency systematic error of 30% (Albert et al. 2008a). For each limit, a power law energy spectrum with a photon index of -2 is assumed both for the simulation of the effective area, and the conversion of event number upper limits to *flux* upper limits. The influence of this photon index is minor, since the energy ranges are sufficiently small.

Finally, since the data can only be selected by *estimated* energy, a Monte Carlo simulation (MC) is used to estimate the median *true* energy of the data that remains after all cuts.

This analysis assumes a source extension similar or smaller than the point spread function (PSF) of MAGIC. In an identically conducted analysis of contemporary Crab Nebula data the width of this PSF (defined as the Sigma of a two dimensional Gaussian function) was found to be

about $0.08°$. Since the Milagro source may be extended, a second analysis was done, assuming an extension of $0.3°$ instead. Since this is done simply by increasing the signal integration radius, more background events are included, which leads to higher upper limits.

4. Discussion

The derived 95% c.l. flux upper limits are summarized in Table 1. Figures 2 and 3 display them in the context of the published satellite data and the Milagro flux estimation. The differences between the limits of J1954 and J1958 are all compatible with the statistical fluctuations that can be expected for 95% upper limits. Around 1 TeV, where MAGIC is most sensitive, the flux is limited to 3% of the Crab Nebula flux for J1954 and 2% for J1958. Assuming that the Milagro emissions originate from objects spacially coinciding with the Fermi pulsars within our PSF, the photon index in the energy range of 1 to 35 TeV must be harder than 2.2 for J1954, and 2.1 for J1958. The spectral energy distribution is thus likely to peak at energies in excess of 1 TeV.

If an extension up to $0.3°$ is assumed, the corresponding flux limits in Crab Nebula units are 14% for J1954 and 3% for J1958. In this extended case, the photon indices are limited to ≤ 2.6 and ≤ 2.2, respectively. It shall be noted that the biggest TeV pulsar wind nebulae have sizes of few tens of parsecs, which at the distance of G65.1+0.6 would be within these $0.3°$.

Bringing together the existing flux data and our upper limits, we conclude that the most likely scenario to explain the gamma ray production measured by Milagro might be the existence of two PWN, associated with the Fermi pulsars. With the ages of the pulsars being 69.5 kyrs and 21 kyrs, it is reasonable to expect an inverse compton component that dominates their energy outflows and may additionally be extended (de Jager & Djannati-Ataï 2009; Tanaka & Takahara 2009). Such old, extended PWN are common TeV gamma-ray sources and frequently have an emission spectrum that peaks at TeV energies or above.

4

5. Summary

We took 25.5 hours of good quality data in the area of the faint supernova remnant G65.1+0.6. In that region, the Milagro collaboration reported the emission of gamma rays with median energy of 35 TeV in the vicinity of the two GeV Fermi pulsars 1FGL J1954.3+2836 and 1FGL J1958.6+2845. Our observations, which were aimed to locate the source of the Milagro emission, yielded no significant gamma-ray signal for these two a-priori known source locations. Also, no post-trial significant signal from a skymap of the area could be established. We extracted three differential flux upper limits for each source, assuming two different extension radii. They are summarized in Figures 2 and 3.

Assuming that the two 4 and 4.3σ detections of Milagro are not statistical fluctuations, but real signals, the flux upper limits support the scenario in which the multi-TeV emission measured by Milagro is caused by a different mechanism or object than the Fermi emission. Given the ages of the pulsars and the SNR, the existence of two very old pulsar wind nebulae, powered by the two GeV pulsars, seems very likely.

REFERENCES

Abdo, A. et al. 2009a, ApJ, 700, L127

Abdo, A. et al. 2009b, ApJS, 183, 46

Abdo, A. et al. 2009c, Science, 325, 840

Abdo, A. et al. 2010a, ApJS, 187, 460

Abdo, A. et al. 2010b, ApJS, 188, 405

Albert, J. et al. 2008a, ApJ, 674, 1037

Albert, J. et al. 2008b, Nucl. Instr. Meth. A, 588, 424

Aliu, E. et al. 2009, Astropart. Phys.,30, 293

Arquilla, R., & Kwok, S. 1987, A&A, 173, 271

Fomin, V. P., Stepanian, A. A., Lamb, R. C., Lewis, D. A., Punch, M., Weekes, T. C. 1994, Astropart. Phys., 2, 137

Hartman, R.C. 1999, ApJS, 123, 79

Landecker, T.L., Clutton-Brock, M., & Purton, C.R. 1990, A&A, 232, 207

de Jager, O.C., & Djannati-Ataï, A. 2009, Neutron Stars and Pulsars (Berlin, Heidelberg: Springer)

Lorimer, D.R., Lyne, A.G., & Camilo, F. 1998, 331, 1002

Moralejo, A. et al. 2009, in Proc. 31st ICRC (Łódź), preprint arXiv:0907.0943

Rolke, W.A., Lopez, A.M., Conrad, J. 2005, Nucl. Instr. Meth. A, 551, 493

Saz Parkinson, P.M. et al. 2010, submitted to ApJ, preprint arXiv:1006.2134v1

Seiradakis, J. H., Reich, W., Sieber, W., Schlickeiser, R., & Kühr, H. 1985, A&A, 143, 478

Swanenburg, B.N. et al. 1981, ApJ, 243, L69

Tanaka, S.J., Takahara, F. 2009, in Proc. 2009 Fermi Symposium (Washington, DC), preprint arXiv:1001.2360
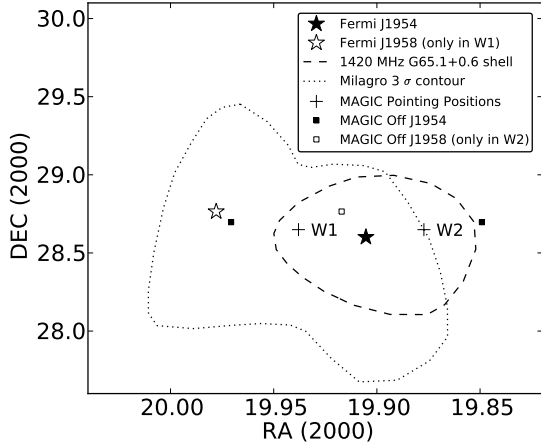
Tian, W.W., & Leahy, D.A. 2006, A&A, 455, 1053

Fig. 1.— Observation setup for the two Fermi sources J1954 and J1958 in the context of SNR G65.1+0.6 and a Milagro significance contour. J1958 appears only in one wobble position (W1), so the OFF data is taken from the other wobble sample, using the same position relative to the pointing direction. The outline of the remnant is taken from the radio map in Landecker et al. (1990). The extension of the Milagro significance contour (Abdo et al. 2009a) is compatible with their point spread function.
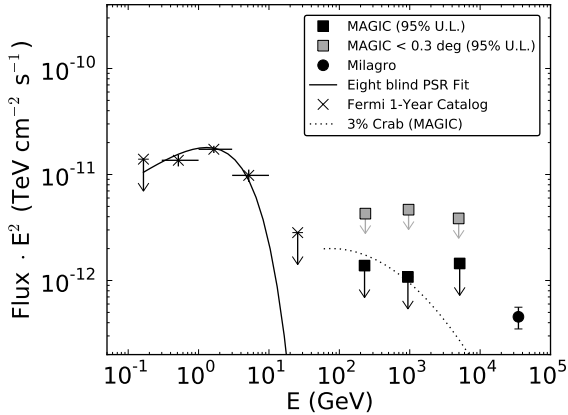

Fig. 2.— Compilation of flux measurements and upper limits for 1FGL J1954.3+2836 from Fermi (Saz Parkinson et al. 2010; Abdo et al. 2010b), MAGIC and Milagro (Abdo et al. 2009a). The 3% fraction of the MAGIC Crab spectrum (Albert et al. 2008a) is shown for comparison.
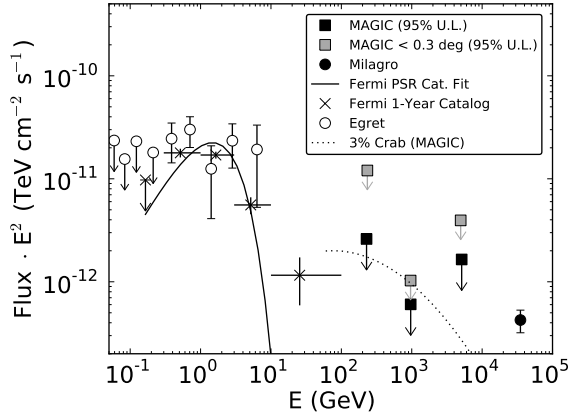

Fig. 3.— Compilation of flux measurements and upper limits for 1FGL J1958.6+2845 from EGRET (Hartman et al. 1999), Fermi (Abdo et al. 2010a,b), MAGIC and Milagro (Abdo et al. 2009a). The 3% fraction of the MAGIC Crab spectrum (Albert et al. 2008a) is shown for comparison.

TABLE 1

DIFFERENTIAL UPPER LIMITS

Source Name	Assumed Extension (deg)	E_{med} (GeV)	Significance (σ)	$F_{95\%}$ ($10^{-12}\,\mathrm{TeV^{-1}cm^{-2}s^{-1}}$)	$F_{95\%}E^2$ ($10^{-12}\,\mathrm{TeVcm^{-2}s^{-1}}$)
1FGL J1954.3+2836	$\leq 0.08°$	228	-1.8	27	1.38
		942	+1.1	1.22	1.08
		5123	+1.9	0.055	1.45
	$\leq 0.3°$	234	-1.3	78	4.3
		963	+2.6	5.0	4.66
		4956	+2.0	0.157	3.85
1FGL J1958.6+2845	$\leq 0.08°$	228	-1.5	50	2.60
		966	-0.9	0.65	0.60
		5123	+0.9	0.063	1.65
	$\leq 0.3°$	234	-0.3	220	12.0
		963	-1.9	1.11	1.03
		4956	+0.8	0.161	3.9